Gain-of-function mutation in Na$_v$1.7 in familial erythromelalgia induces bursting of sensory neurons

S. D. Dib-Hajj,[1,2,3] A. M. Rush,[1,2,3] T. R. Cummins,[4] F. M. Hisama,[1] S. Novella,[1] L. Tyrrell,[1,2,3] L. Marshall[1] and S. G. Waxman[1,2,3]

[1]Department of Neurology and [2]Center for Neuroscience and Regeneration Research, Yale University School of Medicine, New Haven, [3]Rehabilitation Research Center, VA Connecticut Healthcare System, West Haven, CT and [4]Department of Pharmacology and Toxicology, Stark Neurosciences Institute, Indiana University School of Medicine, Indianapolis, IN, USA

Correspondence to: Stephen G. Waxman, MD, PhD, Department of Neurology, LCI 707, Yale School of Medicine, 333 Cedar Street, New Haven, CT 06510, USA
E-mail: stephen.waxman@yale.edu

Erythromelalgia is an autosomal dominant disorder characterized by burning pain in response to warm stimuli or moderate exercise. We describe a novel mutation in a family with erythromelalgia in SCN9A, the gene that encodes the Na$_v$1.7 sodium channel. Na$_v$1.7 produces threshold currents and is selectively expressed within sensory neurons including nociceptors. We demonstrate that this mutation, which produces a hyperpolarizing shift in activation and a depolarizing shift in steady-state inactivation, lowers thresholds for single action potentials and high frequency firing in dorsal root ganglion neurons. Erythromelalgia is the first inherited pain disorder in which it is possible to link a mutation with an abnormality in ion channel function and with altered firing of pain signalling neurons.

Introduction

Sodium channels contribute to dorsal root ganglion (DRG) neuron hyperexcitability associated with acquired pain (Waxman *et al.*, 1999; Black *et al.*, 2002), but their role in hereditary pain syndromes is less well understood. Primary erythromelalgia (also called primary erythermalgia) is an autosomal dominant painful neuropathy with characteristics that include burning pain of the extremities in response to warm stimuli or moderate exercise (van Genderen *et al.*, 1993). Recently, two mutations in *SCN9A*, the gene for the human Na$_v$1.7 sodium channel, were reported in primary erythromelalgia (Yang *et al.*, 2004). Na$_v$1.7 channels are preferentially expressed in nociceptive DRG neurons and sympathetic ganglion neurons (Sangameswaran *et al.*, 1997; Toledo-Aral *et al.*, 1997; Djouhri *et al.*, 2003), and produce 'threshold currents' close to resting potential, amplifying small depolarizations such as generator potentials (Cummins *et al.*, 1998), while other sodium channel isoforms contribute most of the current

underlying all-or-none action potentials in DRG neurons (Renganathan *et al.*, 2001; Blair and Bean, 2002). The previously described mutations of Na$_v$1.7 cause a 13–15 mV hyperpolarizing shift in activation, slow deactivation and increase the response of the channels to small ramp depolarizations (Cummins *et al.*, 2004). We now describe a third mutation in Na$_v$1.7 which segregates with the disease phenotype in a large pedigree of primary erythromelalgia, describe its effects on channel function and show, for the first time, that a mutation in a human sodium channel can lower the threshold for single action potentials and high frequency firing of DRG neurons.

Subjects and methods
Patients
A neurologist blinded to the genetic studies confirmed disease phenotype, based on formal clinical criteria (Drenth and Michiels,

1994), in 17 affected subjects, five unaffected subjects and three unaffected spouses after informed consent was obtained. In a study approved by the Yale Medical School Human Investigation Committee. A clinical description for part of this family (Finley *et al.*, 1992) and linkage to chromosome 2q31–q32 have been reported (Drenth *et al.*, 2001), but detailed genetic analysis had not been carried out previously.

Exon screening

Genomic DNA was purified from buccal swabs or venous blood from 25 family members (17 affected; eight unaffected). Human variation panel control DNA (25 males, 25 females; Caucasians) was obtained from the Coriell Institute (Camden, NJ). The genomic sequence of SCN9A (GenBank accession no. NC_000002) was used to design intron-specific primers to amplify coding and non-coding exons which produce $Na_v1.7$ cDNA. Genomic sequences were compared with the reference $Na_v1.7$ cDNA (Klugbauer *et al.*, 1995) to identify sequence variation. Sequencing was performed at the Howard Hughes Medical Institute/Keck Biotechnology Center at Yale University. Sequence analysis used BLAST (National Library of Medicine) and Lasergene (DNAStar, Madison, WI).

Voltage-clamp analysis

The plasmid carrying the TTX-R version of human $Na_v1.7$ cDNA ($hNa_v1.7_R$) was described previously (Herzog *et al.*, 2003). The F1449V mutation was introduced into $hNa_v1.7_R$ using QuickChange XL site-directed mutagenesis (Stratagene, La Jolla, CA). Wild-type or F1449V mutant $hNa_v1.7_R$ channels were co-transfected with the human β1 and β2 subunits (Lossin *et al.*, 2002) into HEK293 cells, grown under standard culture conditions (5% CO_2, 37°C) in Dulbecco's modified Eagle's medium supplemented with 10% fetal bovine serum, by calcium phosphate precipitation (Cummins *et al.*, 2004).

Whole-cell patch-clamp recordings were conducted at room temperature (~21°C), 40–72 h after transfection using an EPC-10 amplifier and Pulse 8.5 (HEKA, Germany) with 0.8–1.5 MΩ electrodes (access resistance 1.6 ± 0.3 MΩ). Voltage errors were minimized using 80% series resistance compensation and linear leak subtraction; capacitance artefact was cancelled using computer-controlled circuitry. Recordings were started 3.5 min after establishing whole-cell configuration. The pipette solution contained: 140 mM CsF, 1 mM EGTA, 10 mM NaCl and 10 mM HEPES (pH 7.3). The bathing solution was 140 mM NaCl, 3 mM KCl, 1 mM $MgCl_2$, 1 mM $CaCl_2$ and 10 mM HEPES (pH 7.3). Data were analysed using Pulsefit (HEKA) and Origin (Microcal, Northampton, MA) software.

Transfection of DRG neurons and current-clamp recordings

DRG from wild-type C57/BL6 mice were treated (Rizzo *et al.*, 1994) to obtain neurons for electroporation of sodium channel and green fluorescent protein (GFP) constructs (Amaxa Inc., Gaithersburg, MD; see on-line Supplementary material available at *Brain* Online). Current-clamp recordings were obtained 16–24 h post-transfection.

Whole-cell current-clamp recordings from small diameter DRG neurons (<30 μm) with robust GFP fluorescence were obtained at room temperature (~21°C) following transfection with either wild-type $hNa_v1.7_R$–GFP or F1449V–GFP using an Axopatch 200B amplifier (Axon Instruments, Union City, CA). Micropipettes with resistances from 1 to 2.5 MΩ were filled with a solution of 140 mM KCl, 0.5 mM EGTA, 5 mM HEPES, 3 mM Mg-ATP and 3 mM Na-GTP, pH 7.3, adjusted to 315 mOsm/l with glucose. The external solution contained 140 mM NaCl, 3 mM KCl, 2 mM $MgCl_2$, 2 mM $CaCl_2$, 10 mM HEPES, pH 7.3, adjusted to 320 mOsm/l with glucose. The pipette potential was adjusted to zero before seal formation; liquid junction potentials were not corrected. Capacity transients were cancelled before switching to current-clamp mode, and series resistance (~3–6 MΩ) was compensated by ~70%. Traces were acquired from cells with stable resting potentials less than −40 mV using Clampex 8.1 software, filtered at 5 kHz and sampled at 20 kHz. When required, steady polarizing currents were applied to set a holding potential of −60 mV.

Results
Clinical description

The pedigree of this family contains 36 members (Fig. 1); 16 subjects with the erythromelalgia phenotype (mean age 37 years; range 3–75) were clinically evaluated (10 women, six men). Mean age of onset of symptoms was 3 years; four patients had onset in infancy, and all had onset of symptoms by their sixth birthday. All subjects experienced symptoms typical of erythromelalgia (Drenth and Michiels, 1994), with attacks of burning pain and erythema involving both surfaces of the hands, and feet up to or slightly proximal to the ankles. Ten subjects (63%) reported involvement of other areas, including face, ears, elbows and knees; one reported involvement of the vaginal area. Eleven (69%) reported attacks one or more times per day; three (19%) reported several attacks per month. All subjects but one (94%) reported that attacks are triggered
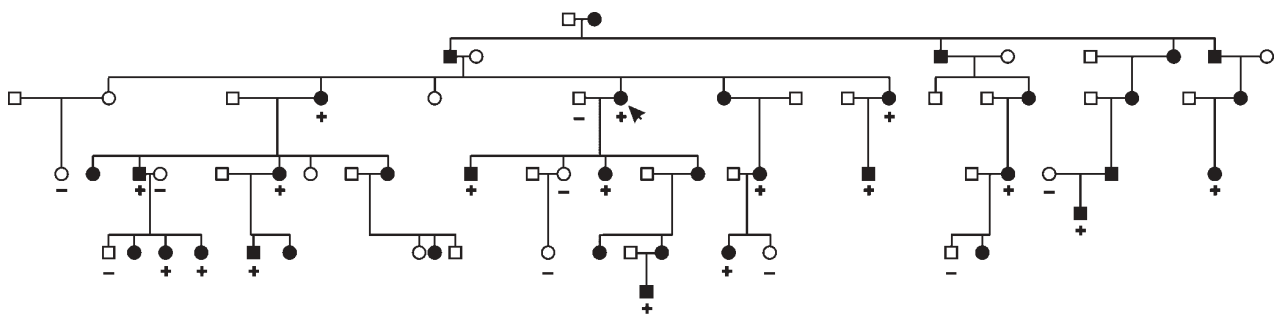

Fig. 1 Family pedigree. Circles denote females; squares denote males. The proband is shown by an arrow. Blackened symbols indicate subjects affected with erythromelalgia. (+) denotes subjects heterozygous for the T4393G mutation; (−) denotes subjects without the mutation.

by heat and improved by cold, although one reported that extreme cold can also trigger attacks.

Mutation in exon 23

Genomic DNA from the proband and control subjects was isolated from venous blood samples and used as template to

```
                                       ↓
Na,1.1  LYMYLYFVIFIIFGSFFTLNLFIGVIIDNFNQQKKKFGGQDIFMTEE
Na,1.2  LYMYLYFVIFIIFGSFFTLNLFIGVIIDNFNQQKKKFGGQDIFMTEE
Na,1.3  LYMYLYFVIFIIFGSFFTLNLFIGVIIDNFNQQKKKFGGQDIFMTEE
Na,1.4  LYMYLYFVIFIIFGSFFTLNLFIGVIIDNFNQQKKKLGGKDIFMTEE
Na,1.5  LYMYIYFVIFIIFGSFFTLNLFIGVIIDNFNQQKKKLGGQDIFMTEE
Na,1.6  IYMYIYFIIFIIFGSFFTLNLFIGVIIDNFNQQKKKFGGQDIFMTEE
Na,1.7  LYMYLYFVVFIIFGSFFTLNLFIGVIIDNFNQQKKKLGGQDIFMTEE
Na,1.8  VYMYLYFVIFIIFGGFFTLNLFVGVIIDNFNQQKKKLGGQDIFMTEE
Na,1.9  SLGYIYFVVFIIFGSFFTLNLFIGVIIDNFNQQQKKLGGQDIFMTEE
Na,1.7m LYMYLYFVIFIIFGSFFTLNLFIGVIIDNᵥNQQKKKFGGQDIFMTEE
        ────────────────────────────    ─────
                 DIII-S6            *
```

Fig. 2 F1449 (arrow) is conserved within loop 3 in all known sodium channels. The lower line delineates the sequence of transmembrane segment S6 of domain III and the N-terminal half of L3 for Na$_v$1.1–Na$_v$1.9, together with the F1449V mutation (Na$_v$1.7 m). The asterisk denotes the position of V1293 which is replaced with isoleucine (I) in the skeletal muscle disorder paramyotonia congenita (Green *et al.*, 1998). The fast inactivation tripeptide IFM is underlined.

amplify all known exons of *SCN9A* and compare the sequence with Na$_v$1.7 cDNA (Klugbauer *et al.*, 1995). Proband and control templates produced similar amplicons which were purified and sequenced. Sequence analysis identified a T-to-G transversion in exon 23 (E23), corresponding to position 4393 of the reference sequence (see Supplementary material). This mutation substitutes phenylalanine (F) by valine (V) at position 1449 of the polypeptide, located at the N-terminus of loop 3 which joins domains III and IV. F1449 is invariant in all known mammalian sodium channels (Fig. 2). Restriction digestion analysis (see Supplementary material) confirmed the presence of the F1449V mutation in 17 out of 17 affected individuals, and its absence in five out of five unaffected family members, three out of three unaffected spouses and 100 ethnically matched control chromosomes. Segregation of the T4393G mutation with disease was confirmed by DNA sequencing of E23 in all family members.

Voltage-clamp analysis

Wild-type hNa$_v$1.7$_R$ and the mutant channel F1449V were transiently expressed along with β1 and β2 subunits (Lossin *et al.*, 2002) in HEK293 cells (Fig. 3A), where Na$_v$1.7 displays biophysical properties (Cummins *et al.*, 1998) similar to those in DRG neurons (Herzog *et al.*, 2003). We examined the
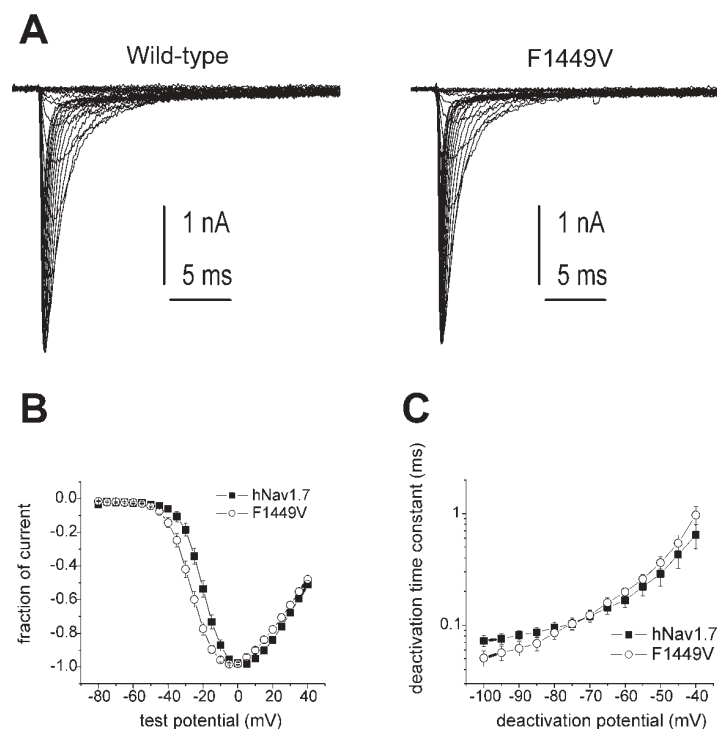

Fig. 3 The F1449V mutation alters activation but not deactivation of hNa$_v$1.7. (**A**) Current traces recorded from representative HEK293 cells expressing either wild-type (left) or F1449V (right) channels. Cells were held at −100 mV and currents elicited with 50 ms test pulses to −80 to +40 mV. (**B**) Normalized peak current–voltage relationship for wild-type (filled squares, $n = 11$) and F1449V (open circles, $n = 12$) channels. (**C**) Time constants for tail current deactivation at repolarization potentials from −40 to −100 mV for wild-type (filled squares, $n = 8$) and F1449V (open circles, $n = 7$) channels. Time constants were obtained with single exponential fits. Error bars show standard errors.

voltage dependence of activation using depolarizing test pulses from −100 mV. Mutant channels activated at potentials 5–10 mV more negative than wild-type channels (Fig. 3B). The midpoint of activation for F1449V (estimated by fitting with a Boltzmann function) was significantly shifted to −22.8 ± 1.3 mV ($n = 12$) compared with wild-type currents (−15.2 ± 1.3 mV, $n = 11$; $P < 0.05$), a smaller shift than for the previously described $Na_v1.7$ mutations (Cummins *et al.*, 2004). The time course of activation, estimated using a Hodgkin–Huxley fit of currents elicited with a step depolarization to −20 mV, was not significantly different for wild-type ($\tau = 482 \pm 25$ μs) and F1449V channels ($\tau = 431 \pm 17$ μs). Deactivation kinetics, examined by eliciting tail currents at different potentials after briefly activating the channels (at −20 mV for 0.5 ms), were not altered at potentials ranging from −100 to −40 mV for the F1449V mutant channel (Fig. 3C), in contrast to the previously described $Na_v1.7$ mutations where deactivation was slower.

Steady-state fast inactivation of F1449V channels (Fig. 4A) was shifted slightly in the depolarizing direction. The $V_{1/2}$ measured with 500 ms pre-pulses was −71.3 ± 0.8 mV for wild-type ($n = 16$) and −67.0 ± 1.4 mV for F1449V ($n = 16$; $P < 0.05$) channels. Voltage dependence of steady-state slow inactivation was shifted in the negative direction by the F1449V mutation (Fig. 4B).

The time constants for open state inactivation (Fig. 4C) were smaller for F1449V than for wild-type currents over the entire voltage range from −50 to +40 mV. At −10 mV, wild-type currents inactivated with a $\tau = 1.4 \pm 0.1$ ms ($n = 7$) and F1449V currents inactivated with a significantly smaller ($P < 0.05$) $\tau = 1.0 \pm 0.2$ ms ($n = 8$). Development of closed state inactivation was faster for F1449V channels, with significantly smaller ($P < 0.05$) time constants for inactivation at −80, −70 and −60 mV (Fig. 4D). Repriming (recovery from fast inactivation) was significantly faster ($P < 0.05$) for F1449V channels than for wild-type channels (Fig. 5A).
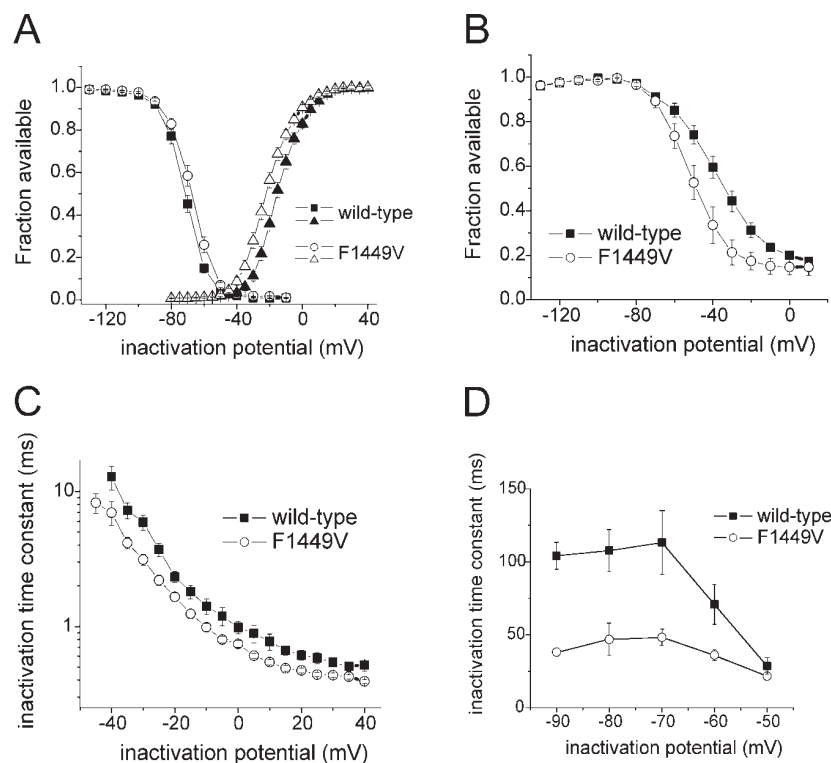

Fig. 4 The F1449V mutation differentially alters fast and slow inactivation of $hNa_v1.7$. (**A**) Comparison of steady-state fast inactivation for wild-type (filled squares, $n = 13$) and F1449V (open circles, $n = 14$) channels. Currents were elicited with test pulses to 0 mV following 500 ms inactivating pre-pulses. The voltage dependence of activation, derived by fitting Boltzmann functions to the data shown in Fig. 3, is shown for wild-type (closed triangles) and F1449V (open triangles). (**B**) Comparison of steady-state slow inactivation for wild-type (filled squares, $n = 4$) and F1449V (open circles, $n = 4$) channels. Slow inactivation was induced with 30 s pre-pulses, followed by 100 ms pulses to −120 mV to allow recovery from fast inactivation. A 20 ms test pulse to 0 mV was used to determine the fraction of current available. (**C**) Fast inactivation kinetics as a function of voltage for wild-type (filled squares, $n = 7$) and F1449V (open circles, $n = 8$) channels. The decay phases of currents elicited as described in Fig. 3A were fitted with single exponentials to estimate open state inactivation time constants. (**D**) Time constants for development of closed state inactivation were estimated from single exponential fits to time courses measured at inactivation potentials from −90 to −50 mV for wild-type (filled squares, $n = 6$) and F1449V channels (open circles, right; $n = 9$), by holding cells at −100 mV, pre-pulsing to the inactivation potential for increasing durations, then stepping to 0 mV to determine the fraction of current inactivated during the pre-pulse. Development of closed state inactivation for F1449V currents is faster than for wild-type currents.
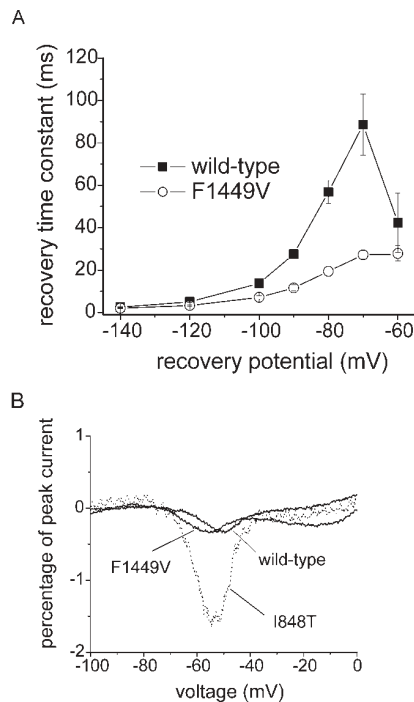
A

B

Fig. 5 Recovery from inactivation kinetics is faster for F1449V mutant channels than for wild-type channels. (**A**) Time constants for recovery from inactivation of wild-type (filled squares, n = 8) and F1449V (open circles, n = 8) currents are shown as a function of voltage. Time constants were estimated from single exponential fits to time courses measured at recovery potentials from −140 to −60 mV, by pre-pulsing the cell to +20 mV for 20 ms to inactivate all of the current, then stepping back to the recovery potential for increasing recovery durations prior to the test pulse to 0 mV. The maximum pulse rate was 0.5 Hz. (**B**) Representative ramp currents, elicited with 500 ms ramp depolarizations from −100 to 0 mV for wild-type and mutant F1449V. The increase in ramp current amplitude, seen for the previously described I848T mutation (Cummins *et al.*, 2004), is not observed.

The time constant for repriming of wild-type channels ($\tau = 89 \pm 14$ ms, n = 8) was 3-fold larger at −70 mV than for F1449V channels ($\tau = 27 \pm 2$ ms, n = 8).

Ramp currents (Fig. 5B), elicited with slow (0.2 mV/ms) depolarizations from −100 to +20 mV, were not different for F1449V channels ($0.4 \pm 0.1\%$; n = 7) and wild-type channels ($0.4 \pm 0.1\%$; n = 12). In contrast, the I848T and L858H hNa$_v$1.7 erythromelalgia mutations elicited significantly larger ramp currents compared with wild-type channels (Cummins *et al.*, 2004).

Current-clamp analysis

Reasoning that changes in voltage dependence could lower the firing threshold, we expressed wild-type or F1449V channels in small (<30 μm) DRG neurons which include nociceptors. Resting potential was similar ($P > 0.05$) in DRG neurons transfected with F1449V (-51.3 ± 1.6 mV; n = 19) and with wild type (-49.0 ± 1.3 mV; n = 16). To eliminate cell-to-cell variations, cells were held at −60 mV.

Na$_v$1.7 is important in early phases of electrogenesis in DRG neurons, producing graded depolarizations which may boost subthreshold inputs (Cummins *et al.*, 1998) to bring DRG neurons to voltages at which Na$_v$1.8 [which has a more depolarized activation threshold (Akopian *et al.*, 1996)] opens to produce all-or-none action potentials (Renganathan *et al.*, 2001). Figure 6A, B and E shows the effect of the F1449V mutation on the firing threshold. Figure 6A shows traces from a representative DRG neuron expressing wild-type hNa$_v$1.7. Subthreshold responses, which depolarized the cell slightly but not to −19 mV where an action potential is triggered, were elicited with 50–65 pA current injections. All-or-none action potentials required stimuli of ≥130 pA (current threshold for this neuron). In contrast, Fig. 6B shows responses from a representative DRG neuron expressing F1449V, where action potentials were produced at a lower current threshold of 60 pA. Current threshold (current required to generate an all-or-none action potential) was significantly reduced ($P < 0.05$) following expression of F1449V (93.1 ± 12.0 pA; n = 19) compared with wild-type (124.1 ± 7.4 pA; n = 16) (Fig. 6E). However, the voltage at which takeoff occurs for an all-or-none action potential was not significantly different ($P > 0.5$) in cells expressing wild-type (-21.4 ± 0.9 mV; n = 16) or F1449V channels (-22.5 ± 1.4 mV; n = 19).

Similarly to native small DRG neurons, ∼50% of which fire repetitively in response to prolonged stimuli (Renganathan *et al.*, 2001), the majority of neurons expressing wild-type Na$_v$1.7 (11 out of 16; 69%) or the F1449V channel (12 out of 19; 63%) can fire repetitively (Fig. 6C and D). Figure 6C shows the firing of a representative neuron expressing wild-type channels, which responded to a 950 ms stimulation of 150 pA with two action potentials. In contrast, a neuron expressing F1449V responds to an identical 150 pA depolarizing stimulus with high frequency firing (Fig. 6D). The firing frequency evoked with 100 pA current injections was increased from 1.24 ± 0.58 Hz (n = 11) for wild-type to 5.34 ± 1.21 Hz (n = 12; $P < 0.01$) for F1449V channels. Current injection of 150 pA evoked firing at 3.03 ± 0.75 Hz (n = 9) following expression of wild-type and 6.48 ± 1.41 Hz (n = 12; $P < 0.05$) following expression of F1449V channels (Fig. 6F). Thus, in addition to a lower current threshold for action potentials, the frequency of firing at graded stimulus intensities was higher for cells expressing F1449V.

Discussion

This study demonstrates, in a large family with primary erythromelalgia, a single substitution of phenylalanine by valine (F1449V) at codon 1449 in the sodium channel Na$_v$1.7. This single amino acid substitution alters the biophysical properties of hNa$_v$1.7 and reduces the threshold for action potential firing and bursting of DRG neurons. F1449 is located within L3, the cytoplasmic loop which joins domains III and IV, 11 amino acid residues N-terminal to the fast inactivation IFM (isoleucine– phenylalanine–methionine) motif (West *et al.*,
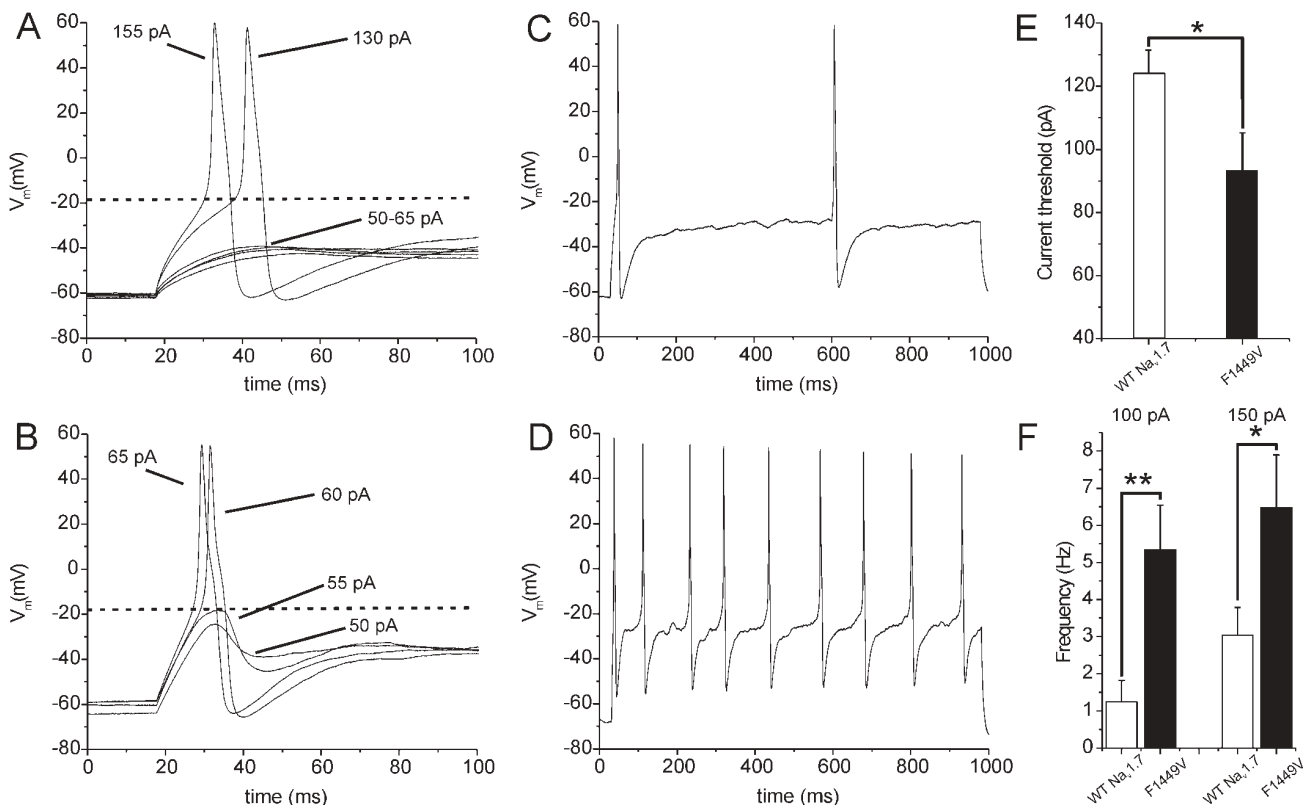
Fig. 6 F1449V, expressed in small DRG neurons, lowers the current threshold for action potential generation and repetitive firing. Action potentials were evoked using depolarizing current injections from a membrane potential of −60 mV. (**A**) Representative traces from a cell expressing wild-type $Na_v1.7$, showing subthreshold responses to 50–65 pA current injections and subsequent all-or-none action potentials evoked by injections of 130 pA (current threshold for this neuron) and 155 pA. (**B**) In contrast, in a cell expressing F1449V, action potentials were evoked by a 60 pA current injection, demonstrating a lower current threshold for action potential generation. The voltage for take off of the all-or-none action potential (dotted line) was similar for the neurons in (**A**) and (**B**). (**C** and **D**) The frequency of firing at graded stimulus intensities was higher for cells expressing F1449V mutant channels than with wild-type channels. (**C**) The firing of a neuron expressing $hNa_v1.7$ (same neuron as in **A**), which responded to a 950 ms stimulation of 150 pA with two action potentials. In contrast, **D** shows that, in a neuron expressing the mutant channel F1449V (same cell as in **B**), an identical 150 pA depolarizing stimulus evoked high frequency firing. (**E**) There is a significant (*$P < 0.05$) reduction in current threshold in cells expressing F1449V ($n = 19$) compared with cells expressing wild-type $Na_v1.7$ ($n = 16$). (**F**) There is a significant increase in the frequency of firing in response to 100 and 150 pA stimuli (950 ms) following expression of F1449V ($n = 12$), in comparison with wild-type $Na_v1.7$ ($n = 11, 9$) (**$P < 0.01$; *$P < 0.05$).

1992). F1449V substitution produces an ∼8 mV hyperpolarizing shift in voltage dependence of activation, smaller than the 13–15 mV shifts in the previously described I848T and L858H $hNa_v1.7$ erythromelalgia mutations (Cummins *et al.*, 2004). F1449V substitution also produces an ∼4 mV depolarizing shift in fast inactivation, which is expected to increase the fraction of channels available for activation close to resting potential. Increased overlap between activation and steady-state inactivation for F1449V channels also increases the predicted window current. These changes each would be expected to lower the threshold of nociceptive DRG neurons which express mutant channels. Current-clamp recordings demonstrated, in fact, a lower threshold for single action potentials and high frequency firing in response to graded stimuli in DRG neurons expressing the mutant channel.

The F1449V mutation also changed some $hNa_v1.7$ properties in ways that might decrease excitability, by enhancing slow inactivation and the rate of closed state inactivation.

Because slow closed state inactivation promotes larger ramp currents, F1449V substitution would be expected to attenuate ramp currents. Indeed, in contrast to the I848T and L858H $hNa_v1.7$ erythromelalgia mutations which increased ramp currents (Cummins *et al.*, 2004), F1449V did not alter ramp currents compared with wild-type channels.

Domain III/S6 and the III–IV linker sequences are highly conserved among the known sodium channels. This region is crucial to fast inactivation (Patton *et al.*, 1992), and has been implicated in other inherited disorders of excitability. Several mutations in the skeletal muscle sodium channel ($Na_v1.4$) that underlie myotonic disorders are located in this region. The $Na_v1.4$ V1293I mutation, at a position corresponding to V1444 in $hNa_v1.7$, five amino acids N-terminal to F1449, causes a mild variant of paramyotonia congenita. The functional consequences of the V1293I mutation in $hNa_v1.4$ (Green *et al.*, 1998) are similar to those of F1449V substitution in $hNa_v1.7$. Both mutations shift activation in a

hyperpolarizing direction and inactivation in a depolarizing direction, and accelerate recovery from inactivation. In a model of muscle excitability, V1293I substitution lowered the threshold for action potential generation and caused myotonia; the −6 mV shift in activation was the major factor leading to this enhanced excitability (Green *et al.*, 1998). However, myotonia produced by the Na$_v$1.4-V1293I mutation is often precipitated by cold, whereas cooling reduces pain in most erythromelalgia patients with the F1449V mutation.

Current-clamp recordings demonstrated a lower current threshold for single action potentials and higher frequency firing in response to graded stimuli, in DRG neurons expressing mutant F1449V channels. Thus, even though F1449V displays a shift in activation that is relatively modest, deactivation that is not prolonged and ramp currents that are not enhanced in comparison with previously described mutations in Na$_v$1.7 (Cummins *et al.*, 2004), F1449V substitution imparts a gain-of-function change on DRG neurons, consistent with the autosomal dominant inheritance of familial erythromelalgia (Drenth *et al.*, 2001; Yang *et al.*, 2004) and our finding that affected family members are heterozygous for the mutation. Nevertheless, the inflection in voltage recordings, at which the upstroke of the all-or-none action potentials arose (approximately −20 mV), was essentially the same in neurons expressing wild-type and F1449V channels. This probably reflects the role of Na$_v$1.7 as a 'threshold channel' which activates at more hyperpolarized potentials so as to boost small, slow depolarizing inputs below action potential threshold (Cummins *et al.*, 1998), and the fact that Na$_v$1.8, with a threshold closer to −20 mV (Akopian *et al.*, 1996), generates most of the current underlying the action potential upstroke in DRG neurons (Renganathan *et al.*, 2001; Blair and Bean, 2002).

The present results demonstrate that a sodium channel mutation can reduce the firing threshold and produce abnormal repetitive firing in sensory neurons in an inherited painful syndrome, primary erythromelalgia. Two anecdotal reports describe partial relief from pain in patients with erythromelalgia treated with lidocaine and mexilitine (Kuhnert *et al.*, 1999; Davis and Sandroni, 2002), and a study on four patients reported reduced pain lasting for at least 2 years with oral mexilitine (Legroux-Crespel *et al.*, 2003). Identification of this mutation and its role in the pathophysiology of erythromelalgia suggest that rational treatment with sodium channel blockers may be efficacious in this disorder.

Acknowledgements

References

Akopian AN, Sivilotti L, Wood JN. A tetrodotoxin-resistant voltage-gated sodium channel expressed by sensory neurons. Nature 1996; 379: 257–62.

Black JA, Cummins TR, Dib-Hajj SD, Waxman SG. Sodium channels and the molecular basis for pain. In: Malemberg AB, Chaplan SR, editors. Mechanisms and mediators of neuropathic pain. Basel: Birkhauser Verlag; 2002. p. 23–50.

Blair NT, Bean BP. Roles of tetrodotoxin (TTX)-sensitive Na$^+$ current, TTX-resistant Na$^+$ current, and Ca^{2+} current in the action potentials of nociceptive sensory neurons. J Neurosci 2002; 22: 10277–90.

Cummins TR, Howe JR, Waxman SG. Slow closed-state inactivation: a novel mechanism underlying ramp currents in cells expressing the hNE/PN1 sodium channel. J Neurosci 1998; 18: 9607–19.

Cummins TR, Dib-Hajj SD, Waxman SG. Electrophysiological properties of mutant Nav1.7 sodium channels in a painful inherited neuropathy. J Neurosci 2004; 24: 8232–6.

Davis MD, Sandroni P. Lidocaine patch for pain of erythromelalgia. Arch Dermatol 2002; 138: 17–9.

Djouhri L, Newton R, Levinson SR, Berry CM, Carruthers B, Lawson SN. Sensory and electrophysiological properties of guinea-pig sensory neurones expressing Na(v)1.7 (PN1) Na$^+$ channel alphasubunit protein. J Physiol 2003; 546: 565–76.

Drenth JP, Finley WH, Breedveld GJ, Testers L, Michiels JJ, Guillet G, et al. The primary erythermalgia-susceptibility gene is located on chromosome 2q31–32. Am J Hum Genet 2001; 68: 1277–82.

Drenth JP, Michiels JJ. Erythromelalgia and erythermalgia: diagnostic differentiation. Int J Dermatol 1994; 33: 393–7.

Finley WH, Lindsey JR Jr, Fine JD, Dixon GA, Burbank MK. Autosomal dominant erythromelalgia. Am J Med Genet 1992; 42: 310–5.

Green DS, George AL Jr, Cannon SC. Human sodium channel gating defects caused by missense mutations in S6 segments associated with myotonia: S804F and V1293I. J Physiol (Lond) 1998; 510: 685–94.

Herzog RI, Cummins TR, Ghassemi F, Dib-Hajj SD, Waxman SG. Distinct repriming and closed-state inactivation kinetics of Nav1.6 and Nav1.7 sodium channels in mouse spinal sensory neurons. J Physiol (Lond) 2003; 551: 741–50.

Klugbauer N, Lacinova L, Flockerzi V, Hofmann F. Structure and functional expression of a new member of the tetrodotoxin-sensitive voltage-activated sodium channel family from human neuroendocrine cells. EMBO J 1995; 14: 1084–90.

Kuhnert SM, Phillips WJ, Davis MD. Lidocaine and mexiletine therapy for erythromelalgia. Arch Dermatol 1999; 135: 1447–9.

Legroux-Crespel E, Sassolas B, Guillet G, Kupfer I, Dupre D, Misery L. Treatment of familial erythermalgia with the association of lidocaine and mexiletine. Ann Dermatol Venereol 2003; 130: 429–33.

Lossin C, Wang DW, Rhodes TH, Vanoye CG, George AL Jr. Molecular basis of an inherited epilepsy. Neuron 2002; 34: 877–84.

Patton DE, West JW, Catterall WA, Goldin AL. Amino acid residues required for fast Na$^+$-channel inactivation: charge neutralizations and deletions in the III–IV linker. Proc Natl Acad Sci USA 1992; 89: 10905–9.

Renganathan M, Cummins TR, Waxman SG. Contribution of Nav1.8 sodium channels to action potential electrogenesis in DRG neurons. J Neurophysiol 2001; 86: 629–40.

Rizzo MA, Kocsis JD, Waxman SG. Slow sodium conductances of dorsal root ganglion neurons: intraneuronal homogeneity and interneuronal heterogeneity. J Neurophysiol 1994; 72: 2796–815.

Sangameswaran L, Fish LM, Koch BD, Rabert DK, Delgado SG, Ilnicka M, et al. A novel tetrodotoxin-sensitive, voltage-gated sodium channel expressed in rat and human dorsal root ganglia. J Biol Chem 1997; 272: 14805–9.

Toledo-Aral JJ, Moss BL, He ZJ, Koszowski AG, Whisenand T, Levinson SR, et al. Identification of PN1, a predominant voltage-dependent sodium

channel expressed principally in peripheral neurons. Proc Natl Acad Sci USA 1997; 94: 1527–32.

van Genderen PJ, Michiels JJ, Drenth JP. Hereditary erythermalgia and acquired erythromelalgia. Am J Med Genet 1993; 45: 530–2.

Waxman SG, Dib-Hajj S, Cummins TR, Black JA. Sodium channels and pain. Proc Natl Acad Sci USA 1999; 96: 7635–9.

West JW, Patton DE, Scheuer T, Wang Y, Goldin AL, Catterall WA. A cluster of hydrophobic amino acid residues required for fast Na(+)-channel inactivation. Proc Natl Acad Sci USA 1992; 89: 10910–4.

Yang Y, Wang Y, Li S, Xu Z, Li H, Ma L, et al. Mutations in SCN9A, encoding a sodium channel alpha subunit, in patients with primary erythermalgia. J Med Genet 2004; 41: 171–4.